The RNA-Binding Protein HuR Promotes Cell Migration and Cell Invasion by Stabilizing the β-*actin* mRNA in a U-Rich-Element-Dependent Manner[▽][†]

Virginie Dormoy-Raclet,[1][‡] Isabelle Ménard,[1][‡] Eveline Clair,[1] Ghada Kurban,[2] Rachid Mazroui,[1] Sergio Di Marco,[1] Christopher von Roretz,[1] Arnim Pause,[2] and Imed-Eddine Gallouzi[1]*

Department of Biochemistry, McGill University, Quebec, Canada,[1] and McGill Cancer Center, McGill University, Quebec, Canada[2]

A high expression level of the β-actin protein is required for important biological mechanisms, such as maintaining cell shape, growth, and motility. Although the elevated cellular level of the β-actin protein is directly linked to the long half-life of its mRNA, the molecular mechanisms responsible for this effect are unknown. Here we show that the RNA-binding protein HuR stabilizes the β-*actin* mRNA by associating with a uridine-rich element within its 3′ untranslated region. Using RNA interference to knock down the expression of HuR in HeLa cells, we demonstrate that HuR plays an important role in the stabilization but not in the nuclear/cytoplasmic distribution of the β-*actin* mRNA. HuR depletion in HeLa cells alters key β-actin-based cytoskeleton functions, such as cell adhesion, migration, and invasion, and these defects correlate with a loss of the actin stress fiber network. Together our data establish that the posttranscriptional event involving HuR-mediated β-*actin* mRNA stabilization could be a part of the regulatory mechanisms responsible for maintaining cell integrity, which is a prerequisite for avoiding transformation and tumor formation.

Actin is a major structural protein expressed in all eukaryotic cells, participating in the formation and maintenance of important cellular components, such as extracellular matrix (ECM), cortical actin, stress fibers, and lamellipodia (72). These structures are known to regulate essential cellular processes including cell adhesion, cell migration/movement, cytokinesis, endo-/exocytosis, cell division, signal transduction, mRNA localization, and transcription (3, 13, 26, 55, 59, 71, 73). During the movement of both normal and cancer cells, the actin cytoskeleton is dynamically remodeled, leading to the production of the necessary force needed for cell migration and movement. Cancer cells, however, acquire different ways to move freely within tissues, causing massive invasion and metastasis. Even though the molecular pathways used by malignant cells to invade and to adhere to a given tissue are dictated in part by the cell type and the degree of differentiation, all of these processes are directly affected by the organization of the actin cytoskeleton (73). Therefore, defining the molecular mechanisms that regulate the expression and function of the actin proteins will help in understanding why and how a cell acquires a malignant phenotype.

In higher eukaryotes, actin exists as six isoforms, each of which is encoded by an individual gene (66). These isoforms include skeletal and cardiac muscle α-actin, smooth muscle α- and γ-actin, and the soluble cytoplasmic β- and γ-actin (34). The main characteristics of actin proteins are their ubiquitous

distribution, as well as their stability and high concentration (10). Although the expression of *actin* genes is regulated at the transcriptional level (52), posttranscriptional events, such as the cellular localization of their mRNAs, affect where and how these proteins will be synthesized in the cell (39). Indeed, several groups have demonstrated that whereas β-actin seems to accumulate at the leading edge of migrating cells, γ-actin appears to be restricted to stress fibers (14, 35). Therefore, it has been concluded that the specific localization of each isoform corresponds to the exact location where their mRNAs are targeted for translation (11).

Interestingly, it has been shown that the localization of the β-*actin* mRNA in the vicinity of the leading edge of different cell lines is regulated by a specific sequence in the 3′ untranslated region (3′UTR), the zip code (40) that mediates the interaction with an RNA-binding protein called (zip code-binding protein) (ZBP) (14). Two separate 54-nucleotide and 43-nucleotide regions of the β-*actin* 3′UTR have been identified as the main *cis*-acting elements that mediate this cytoplasmic relocalization (39, 40). Treatment of cells with antisense oligonucleotides directed against the zip code sequence or with a dominant-negative isoform of the ZBP1 protein results in β-*actin* mRNA delocalization and impairment of cellular motility (18, 40). These observations and others establish ZBP1 as an adaptor protein required for the cellular movement of *actin* mRNA (11, 18, 40). However, other RNA-binding proteins, such as hnRNPA2, the KH-type splicing regulatory protein, and one of the brain-specific embryonic lethal abnormal vision (ELAV) proteins, HuC (1), were also shown to associate with the 3′UTR of β-*actin* mRNA. These proteins bind either the zip code sequence (hnRNP A2 and KH-type splicing regulatory protein) or a nearby uridine-rich (U-rich) element (HuC) (54, 62). Therefore, it is possible that these proteins and/or others could either collaborate with ZBP1 to target β-*actin* mRNA to its

---

cellular location or affect other yet-to-be-discovered posttranscriptional events that are required for its processing.

Another important aspect of β-*actin* mRNA is its long half-life (14, 52). Interestingly, although blocking the activity of the ZBP1 protein using a dominant-negative isoform affects β-*actin* mRNA cellular distribution (18), it did not have any impact on its steady-state level, suggesting that the long half-life of this mRNA depends on other yet-unknown *cis*- and *trans*-acting elements. It has been suggested that the β-*actin* 3′UTR could harbor *cis*-acting sequences responsible for the expression of its message (50); however, no information was provided regarding the nature and the protein players that interact with this element. The fact that in rat brain β-*actin* mRNA interacts with the HuC protein (62), which is homologous to the well-characterized mRNA stabilizing factor, HuR (6, 17, 53), led us to hypothesize that these two proteins could both be involved, separately or together, in the stabilization of this message. Unlike the HuC protein, which is expressed exclusively in the brain (1), HuR is expressed ubiquitously at high levels in all organs. HuR was isolated based on its ability to bind specifically the adenosine-uridine-rich elements (AU_3A) (AREs) found in the 3′UTRs of many short-lived mRNAs, such as cytokines, lymphokines, proto-oncogenes, and growth factors (6). The presence of AREs in the 3′UTRs of these labile mRNAs acts as a destabilizing sequence that targets these messages for rapid degradation (12, 61). The half-lives of these mRNAs were shown to increase significantly when they were bound to the HuR protein (17, 53). The HuR protein is predominantly nuclear; however, it can shuttle between the nucleus and the cytoplasm by virtue of its HuR nucleocytoplasmic shuttling domain (16). In addition to its role as an mRNA stabilizer, HuR can also function as an adaptor protein for the nuclear export of many ARE-containing mRNAs, as well as an inhibitor or activator of their translation (5, 6, 24, 42). Although the roles of HuR in key cellular processes, such as cell differentiation (19, 67) and the cell response to stress (22, 44), are well established, its effects on cell migration/movement and cell adhesion remain elusive.

To explore a potential role of HuR in regulating cytoskeletal activities, we used RNA interference to knock down HuR expression in HeLa and WI38 cells. We provide evidence that HuR-deficient cells have reduced adhesive and migratory capacities, accompanied by the inability to assemble actin stress fibers. This reveals a functional link between HuR and the formation and remodeling of actin-based cytoskeletal structures. Since HuR has been shown to associate with β-*actin* mRNA (63), we hypothesized that HuR could be the stabilizing factor that maintains the long half-life of this message. The observations described in this study suggest that the HuR protein plays a major role in cell migration and adhesion, likely by maintaining the stability of the β-*actin* mRNA in a U-rich-element-dependent manner.

MATERIALS AND METHODS

Cell culture and transfection. Adherent HeLa and WI38 cells were maintained in Dulbecco's modified Eagle medium (Sigma, St. Louis, MO) supplemented with 10% (vol/vol) fetal bovine serum (Sigma), glutamine, penicillin, streptomycin, and sodium pyruvate at 37°C in 5%-CO_2 humidified air.

To knock down HuR and β-actin in these cells, we used the small interfering RNA (siRNA) duplexes (67, 31). The experiment was performed as described previously (67) with the following modifications: cells were plated at 2×10^5 cells per well of a 6-well plate and grown overnight at 37°C with 5% CO_2. The

following day, cells were transiently transfected with 0.12 μM of either the control (siCtr) or siRNA directed against *HuR* mRNA (siHuR) or siRNA that targets specifically the β-*actin* message (siβ-actin) in OPTI-MEM I reduced serum medium (Invitrogen, Carlsbad, CA) using Lipofectamine Plus (Invitrogen, Carlsbad, CA) according to the manufacturer's instructions. Cells were processed 72 h posttransfection.

Proliferation determination. HeLa cells (2×10^5) were plated in six-well plates 24 h before the transfection of interfering RNA (RNAi). Control, HuR knockdown, and mock HeLa cells were counted every day following the transfection.

Adhesion, migration, and invasion assay. Six-well plates were coated with 0.1% gelatin or 25 μg/ml fibronectin at 4°C overnight. To avoid nonspecific binding, wells were blocked with 1% bovine serum albumin (BSA) for 1 h at 37°C. Control, HuR knockdown, and mock cells were plated 72 h after the transfection of the RNAi on the matrix-coated wells for 6 h. Adherent cells were fixed with methanol at −20°C and stained with 4′,6′-diamidino-2-phenylindole (DAPI). The nuclei were counted by fluorescence microscopy.

For the migration assay, cell culture filter inserts (8 mm pore; Fisher) were put into 24-well plates to obtain a modified Boyden chamber as described previously (41). Forty-eight hours after the transfection of the siRNA duplexes, the lower reservoir of the chamber was filled with complete medium and the upper reservoir was filled with control, HuR knockdown, and mock HeLa cells resuspended in complete medium (DMEM–10% fetal bovine serum). Cells (10^5) were allowed to migrate through the filter for 22 h at 37°C. Cells that had migrated to the lower surface were fixed using 10% neutral buffered formalin (Surgipath) and stained using 0.1% crystal violet solution (Sigma). Cells were counted using a light microscope. For the invasion assay, the protocol was performed as described previously (43). The results of each one of these experiments were based on 10 different fields.

Measurement of cell growth by MTT assay. The methyl thiazolyl tetrazolium (MTT) cell proliferation assay is a colorimetric assay system which measures the reduction of a tetrazolium component (MTT) into an insoluble formazan product by the mitochondria of viable cells. After incubation of the adherent cells with the MTT reagent, a detergent solution (dimethyl sulfoxide) is added to lyse the cells and solubilize the colored crystals. The samples are read using an enzyme-linked immunosorbent assay plate reader at a wavelength of 570 nm. The amount of color produced is directly proportional to the number of viable and adherent cells.

Simultaneously with the migration assay, the viability and adherence of siHuR- or siCtr-treated cells were measured by the MTT assay. siHuR and siCtr cells were seeded for 6 h at the same concentration as for the migration assay. The medium containing detached cells was removed, and each well was then incubated with MTT for 2 h. The liquid was removed, and dimethyl sulfoxide was added to dissolve the solid residue. The optical density of each well at 570 nm was determined using a microplate reader. MTT is metabolized by the adherent and viable cells to colorimetrically measurable compound.

Immunofluorescence labeling. The cellular localization of proteins of interest was accomplished by indirect immunofluorescence. Briefly, cells were plated on glass coverslips in six-well plates and allowed to attach overnight. After the appropriate experimental treatments (siRNA), cells were rinsed twice in phosphate-buffered saline (PBS), fixed in 3% phosphate-buffered paraformaldehyde, and permeabilized in 0.5% PBS-goat serum with Triton. After permeabilization, cells were incubated with primary antibodies for 1 h at room temperature and then incubated with goat antimouse secondary antibodies conjugated with rhodamine (red) or fluorescein isothiocyanate (FITC) (green) from Molecular Probes (Eugene, OR). To visualize F-actin, cells were stained with FITC-phalloidin (Molecular Probes). Microscopic analyses were performed using an AXIOVERT 200 M microscope (Zeiss).

Preparation of cell extracts and immunoblotting. For the preparation of nuclear and cytoplasmic cell extracts, the PARIS kit (Ambion) was used according to the manufacturer's instructions and 10 μg of proteins were loaded on a 12% sodium dodecyl sulfate (SDS)-polyacrylamide gel. Total cell extracts were prepared as described previously (67).

For immunoblotting, proteins were transferred to nitrocellulose membranes (Bio-Rad, Hercules, CA) and probed with the following antibodies: HuR monoclonal (1:15,000 dilution) (22), antitubulin monoclonal (Sigma) (1:3,000 dilution), anti-β-actin monoclonal (Sigma) (1:2,000 dilution), anti-γ-actin polyclonal (1:10,000 dilution) (Santa Cruz), anti-hnRNPA1 monoclonal (kindly provided by G. Dreyfuss, University of Pennsylvania School of Medicine, Philadelphia; 1:5,000 dilution), and G3BP polyclonal (1:1,000 dilution). Horseradish peroxidase-conjugated goat antimouse and goat antirabbit (Amersham Pharmacia Biotech) were used as the secondary antibodies. Blots were developed with the Amersham Enhance chemiluminescence system.

Immunoprecipitation. (i) Immunoprecipitation of HuR followed by immunoblotting. Cells were lysed in the same buffer as described above. Cell extracts were then incubated by rocking them end-over-end for 2 h at 4°C with 15 μl of monoclonal anti-HuR antibodies or control monoclonal anti-hemagglutinin antibodies (Santa Cruz). Then, 100 μl of a fresh 50% protein A-Sepharose slurry in PBS (Amersham Pharmacia Biotech) was added to each Eppendorf tube and incubated by rocking it end-over-end for 4 h at 4°C. Proteins were then eluted in 150 μl 4× Laemmli sample buffer. Two microliters of total cell extract, supernatant, and immunoprecipitate fractions was loaded on a 12% SDS-polyacrylamide gel and immunoblotted using anti-HuR monoclonal antibodies.

(ii) Immunoprecipitation of HuR followed by reverse transcription (RT)-PCR. Immunoprecipitation and RNA preparation were performed as described previously (63, 67).

RNA extraction, Northern blot analysis, and actinomycin D (ActD) pulse-chase experiments. For fractionation experiments, RNA was extracted from nuclear and cytoplasmic fractions using the PARIS kit (Ambion) according to the manufacturer's instructions. All other RNA extractions were performed using TRIzol reagent (Invitrogen). Northern blot analysis was performed as previously described using 10 μg total RNA (15). After transferring it to a Hybond-N membrane (Amersham) and UV cross-linking, the blot was hybridized with human β-actin or GAPDH cDNA probes generated by random primer labeling (Roche) according to the manufacturer's instructions. The β-actin PCR-amplified fragment that was used to generate the labeled probe was amplified from a plasmid containing the 3′UTR of β-actin mRNA using Taq DNA polymerase (Sigma) and the following oligonucleotides: 5′-GCG CGG ATC CGC GGA CTA TGA CTT AGT TGC G-3′ (forward) and 5′-GCG CGC GGC CGC CCA CAT CGT GAA CTT TGG GGG-3′ (reverse). The glyceraldehyde-3-phosphate dehydrogenase PCR-amplified fragment that was used to generate the labeled probe was amplified from a plasmid containing the glyceraldehyde-3-phosphate dehydrogenase cDNA using Pfu DNA polymerase and the following oligonucleotides: 5′-GCA GGG GGG AGC CAA AAG GG-3′ (forward) and 5′-TGC CAG CCC CAG CGT CAA AG-3′ (reverse).

The stability of β-actin mRNA in HuR RNAi-treated cells and control siRNA-treated cells was assessed by the addition of the general transcriptional inhibitor ActD (5 μg/ml) for the indicated periods of time.

In vitro transcription. Certain β-actin cRNAs were generated from annealed forward and reverse synthetic oligonucleotides fused to a T7 promoter. The following oligonucleotide were used for each of these cRNAs: 5′-GCG GAC TAT GAC TTA GTT GCG TTA CAC CCT TTC TTG ACA AAA CCT AAC TTG C-3′ (forward) for zip code cRNA, 5′-GGC TTT ATT TGT TTT TTT TGT TTT GTT TTG GTT TTT TTT TTT TTG GC-3′ (forward) for probe 2A, 5′-TTG ACT CAG GAT TTA AAA ACT GGA ACG GT-3′ (forward) for probe 2B, 5′-GGC CCC ACC CGT CTC TCT CGT CTC GTC TCG GTC TCT CTC TCT CTC TCG GC-3′ (forward) for probe 2A mutant, 5′-CAG GGG AGG TGA TAG CAT TGC TTT CGT GTA AAT TAT GTA ATG CAA AA-3′ (forward) for probe 4, 5′-TTT TTT TAA TCT TCG CCT TAA TAC TTT TTT ATT TTG TTT TAT TTT GAA TGA TGA GCC-3′ (forward) for probe 5, 5′-TTC GTG CCC CCC CTT CCC CCT TTT TGT CCC CCA ACT TGA GAT GTA TGA A-3′ (forward) for probe 6, 5′-GGC TTT TGG TCT CCC TGG GAG TGG GTG GAG GCA GCC AGG GCT TAC CTG TA-3′ (forward) for probe 7, 5′-CAC TGA CTT GAG ACC AGT TGA ATA AAA GTG CA-3′ (forward) for probe 8, 5′-TGG CTT TAT TTG TTT TTT TTG-3′ (forward) for probe 2AL, 5′-TTT TTT TTG TTT TGT TTT GG-3′ for probe 2AM, 5′-TTT TGT TTT GGT TTT TTT TTT TTT TTT GGC-3′ for probe 2AR, 5′-TGG CTT TAT TTG TTT TTG TTT TTT TGT TTC TTT GGC-3′ for probe 2A mut1, and 5′-TGG CTT TAT TTG TTT TTT TTG TTT TGT TTT GGT TTT TTT TTT TTC TTT GGC-3′ for probe 2A mut2. Oligonucleotide annealing was performed by mixing the forward and reverse oligonucleotides and then cooling to room temperature.

Other β-actin cRNAs were generated from PCR-amplified β-actin 3′UTR regions. The following oligonucleotide pairs were used for each of these cRNAs: 5′-GCA GAA AAC AAC ATG AGA TTG GC-3′ (forward) and 5′-ACC GTT CCA GTT TTT AAA TCC TTG-3′ (reverse) for probe 2 and 5′-GAA GGT GAC AGC AGT CGG TTG-3′ (forward) and 5′-3′ (reverse) for probe 3. Six microliters of annealed oligonucleotides or 0.5 μg of PCR-amplified products were used in an in vitro transcription using the SP6/T7 transcription kit (Roche) according to the manufacturer's instructions. ³²P-labeled and unlabeled cRNAs were then precipitated as previously described (15).

Constructs. A Renilla luciferase cDNA (pRL) under the control of a simian virus 40 promoter (Promega) was used as a reporter gene for the stability experiment. The β-actin-3′UTR, the 2A region, and the 2A-mut region were cloned downstream of the stop codon. The primers used to amplify these three fragments prior to their cloning were described above (see "In vitro transcrip-

tion") with the following modifications. The β-actin 3′UTR was prepared by PCR. Prior to cloning, the pRL plasmid was digested with XbaI and made blunt by the T4 polymerase fill-in reaction. The 2A and 2A-mut fragments were cloned in XbaI and NotI restriction sites. The ActD pulse-chase assay was performed as described above.

Electromobility shift assays. Five micrograms total cell extracts (TCE) or 500 ng purified protein (glutathione S-transferase [GST] or GST-HuR) was incubated with 100,000 cpm of ³²P-labeled cRNAs in a total volume of 20 μl EBMK buffer (25 mM HEPES, pH 7.6, 1.5 mM KCl, 5 mM MgCl₂, 75 mM NaCl, 6% sucrose, and protease inhibitors) at room temperature for 15 min. For competition assays, 0.01×, 0.1×, 1×, 10×, and 100× excess unlabeled specific or unspecific transcripts were incubated with the TCE for 15 min at room temperature before the ³²P-labeled probes were added. Two microliters of a 50-mg/ml heparin sulfate stock solution was then added to the reaction mixture for an additional 15 min at room temperature. In supershift experiments, 5 μg of a purified monoclonal anti-HuR antibody was then added for an additional 15 min at room temperature. Samples were then loaded on a 4% polyacrylamide gel containing 0.05% NP-40.

Microarray analysis. Microarray experiments were performed as described previously (64), using the single-spotted array containing 19,000 probe sets of characterized and unknown human expressed sequence tags from the Health Network Microarray Center, Ontario Cancer Institute, Toronto, Canada. siHuR- or siCtr-treated HeLa cells were grown for 48 h post-transfection of the siRNA duplexes, and total RNAs were prepared and used to produce reverse-transcribed probes. The probing and analysis of cDNA arrays were performed as described previously (64). Using total RNA, the signal for a gene was considered significantly above background levels if the adjusted intensity (total signal minus background) was more than threefold the background signal. Changes in the mRNA profile before and after siHuR treatment were considered significant if they were threefold or greater. Comparison of multiple cDNA array images (two independent experiments) was performed by using an average of all of the gene signals on the array (global normalization) to normalize the signal intensity between arrays.

RESULTS

Knockdown of HuR reduces cell adhesion and slows down its growth rate. While defining the role of the HuR protein in the cell stress response, we observed that depleting its expression from HeLa cells by using the RNA interference technique delayed stress-induced cell death (R. Mazroui, E. Claire, S. DiMario, S. A. Tenenbaum, J. D. Keene, M. Saleh, and I. E. Gallouzi, submitted for publication). The knockdown of HuR in HeLa cells did not induce any cell death; however, it triggered striking morphological changes (Mazroui et al., submitted). We confirmed this effect (Fig. 1A, compare panels a and b) and assessed if these changes reflected an effect on cell behavior. We first investigated the impact of HuR knockdown on cell adhesion and cell proliferation. HeLa cells, transfected with either siCtr or siHuR (67), were harvested and used in an in vitro cell adhesion assay. Seventy-two hours post-transfection of siRNA duplexes, these cells were plated on gelatin or fibronectin for 6 h. The adherence efficiency was defined by calculating the number of HeLa cells that remain attached upon siRNA treatment (see Materials and Methods). We found that the amount of HeLa cells still attached to the matrixes (both gelatin and fibronectin) was reduced by twofold (>50%) in siHuR-treated cells compared to levels for the control (Fig. 1A and B). Since gelatin and fibronectin are known to facilitate the attachment and spreading of HeLa cells (48, 49), our data suggested that the HuR protein is required for efficient cell adhesion.

Usually a defect in an early event during cell growth, such as adhesion, is followed by a slowdown in cell spreading and proliferation (a later event) (58). Since cell proliferation is defined as the time needed for one round of cell division, also

A

Gelatin

siHuR 72h   siCtr 72h

Phase

Fibronectin

SiHuR 72h   SiCtr 72h

Phase

B

C

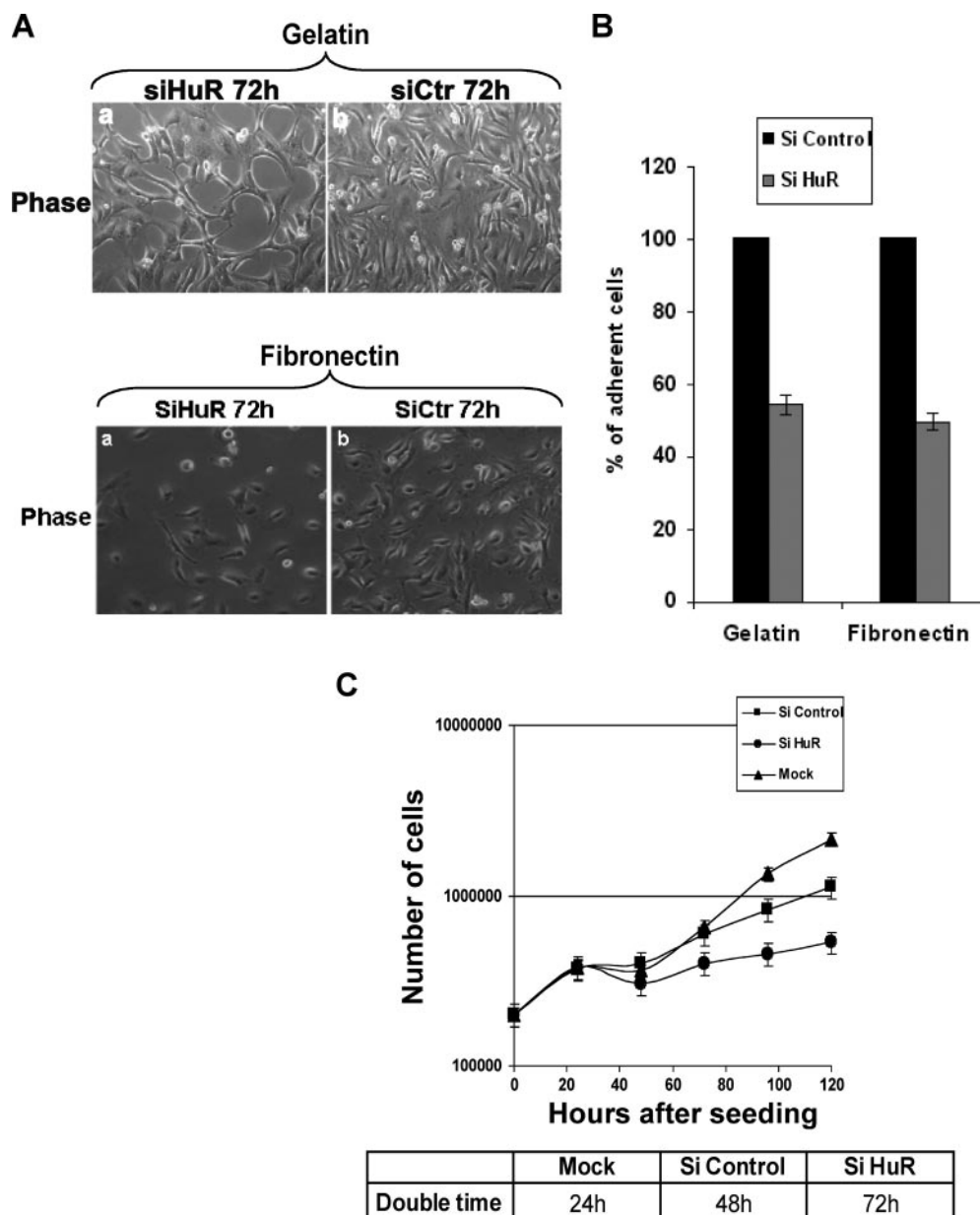| Double time	Mock	Si Control	Si HuR
	24h	48h	72h

FIG. 1. Effect of HuR knockdown on cell growth. (A) Effect of HuR depletion on cell adhesion. HeLa cells transfected with siCtr or siHuR were seeded on six-well plates with gelatin (upper panels) or fibronectin (lower panels). Adherent cells were also stained with DAPI (data not shown). (B) The nuclei were counted by fluorescence microscopy. Relative numbers of cells are shown as means ± standard deviations for three experiments. For each experiment, pictures of 10 fields (equal size) were taken and the cells were counted. (C) Doubling time of HeLa cells knocked down for HuR. HeLa cells (2×10^5) were seeded on six-well plates and then treated with siRNAs as described for panel A. Cells were counted every day for 5 days. Data represent the means ± standard deviations for two independent experiments, each performed in triplicate.

named doubling time, we tested the effect of HuR on this process by determining the growth rate of HeLa cells treated with siHuR or siCtr. Twenty-four hours following the transfection of siRNA duplexes, the cell number was determined every day for 5 days. HeLa cells depleted of the HuR protein showed a doubling time of 72 h, while cells treated with siCtr divided every 48 h (Fig. 1C). However, and as expected, mock-transfected cells presented a doubling time of 24 h, suggesting that the transfection of any siRNA duplexes could have a general

effect on cell growth (Fig. 1C). Nevertheless, the 24-h delay in the growth rate observed for siHuR-treated cells compared to that for siCtr-treated cells indicated that the HuR protein is also involved in cell proliferation.

siRNA-mediated HuR depletion affects cell migration, cell invasion, and formation of stress fibers. It is well established that the composition of the ECM and the concentrations of many of its components determine the adhesion strength, which in turn affects the velocity of a cell during its movement
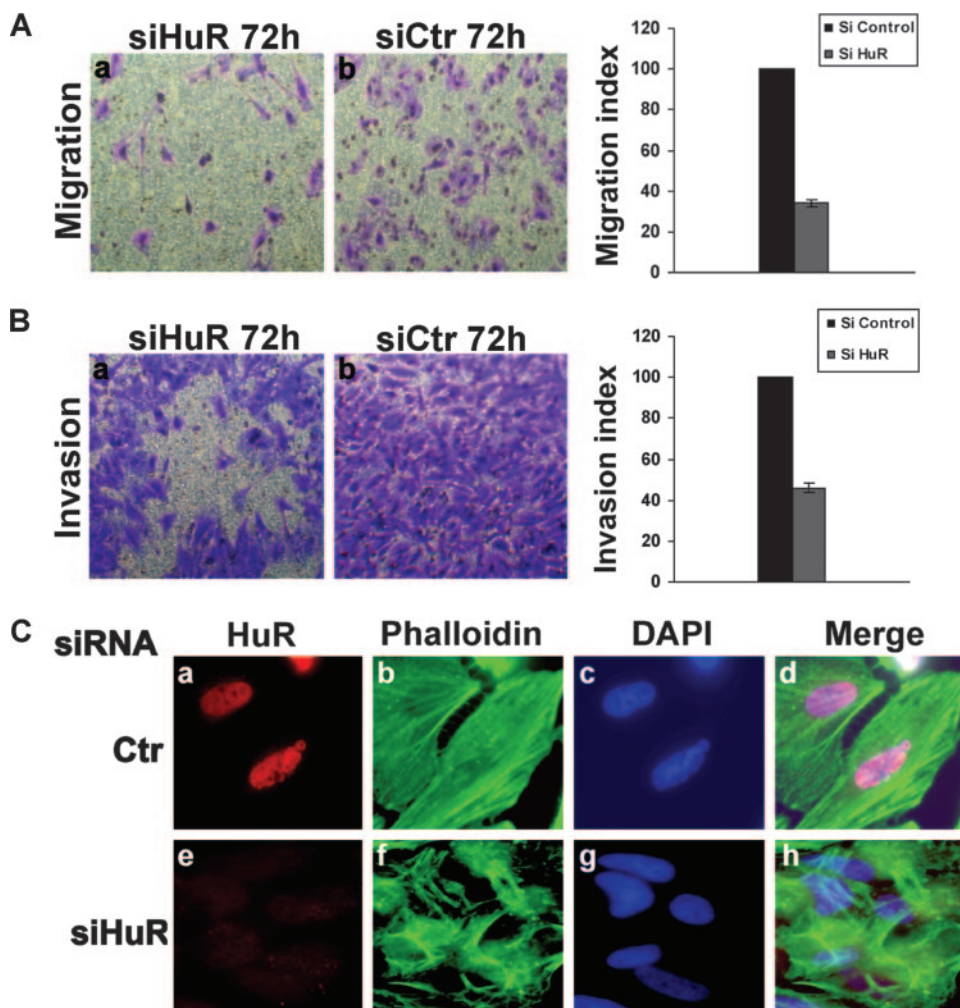
FIG. 2. Effects of HuR knockdown on cell migration, cell invasion, and stress fiber formation. (A) Effects on cell migration. Migration of HeLa cells treated with siHuR or siCtr was analyzed with an uncoated Boyden chamber (left panel). Relative numbers of migrating cells are shown as means ± standard deviations for four experiments (right panel). For each experiment, pictures of 10 fields (equal size) were taken and the cells have been counted. (B) Effect on cell invasion. HeLa cells were transfected with either siHuR or siCtr. After 48 h, the two cell lines were incubated on transwell filters coated with GFR Matrigel for 28 h (left panel). Relative numbers of invading cells are shown as means ± standard deviations for four experiments (right panel). For each experiment, pictures of 10 fields (equal size) were taken and the cells counted. (C) Effect of HuR knockdown on stress fiber formation. HeLa cells were transfected with siHuR or siCtr and then stained with the anti-HuR antibody and FITC-phalloidin.

from one place to another (28, 60). Therefore, if the HuR protein plays a key role in cell behavior, its cellular depletion should also have an impact on cell migration and invasion. To assess this possibility, HeLa cells were transfected with siHuR or siCtr duplexes, and the effect of HuR knockdown on cell migration and cell invasion was defined using the Boyden chamber system (20, 41). This assay was used to determine the number of migratory or invasive cells that cross a polycarbonate transwell filter placed in a 24-well plate. For the migration experiment, the transwell filters were used without any treatment. As shown in Fig. 2A, the number of cells that migrated through this filter was significantly reduced for HuR knockdown cells compared with that for control cells (Fig. 2A). To assess an effect of HuR on invasion, the same assay was performed except that the polycarbonate transwell filters were precoated with GFR Matrigel. We observed that knocking

down the HuR protein resulted in a twofold reduction in the invasiveness of siHuR-treated HeLa cells compared to that of the control (Fig. 2B). To verify that the observed decrease in migration and invasion was not the result of an effect on proliferation and adhesion, we performed the MTT assay to estimate cell viability (cells that remain attached upon siRNA treatment) as described previously (7). The MTT test showed that prior to our migration-and-invasion assays, the numbers of siHuR- and siCtr-treated cells were almost identical. In fact, a difference of less than 5% between siHuR- and siCtr-treated cells allowed us to conclude that the observed effect was due only to an effect on migration or invasion and was not due to a lack of cell adherence (data not shown). These observations suggested that HuR plays an important role in the ability of the cell to move from one place to another.

Cell migration and invasion require a solid cell architecture

A

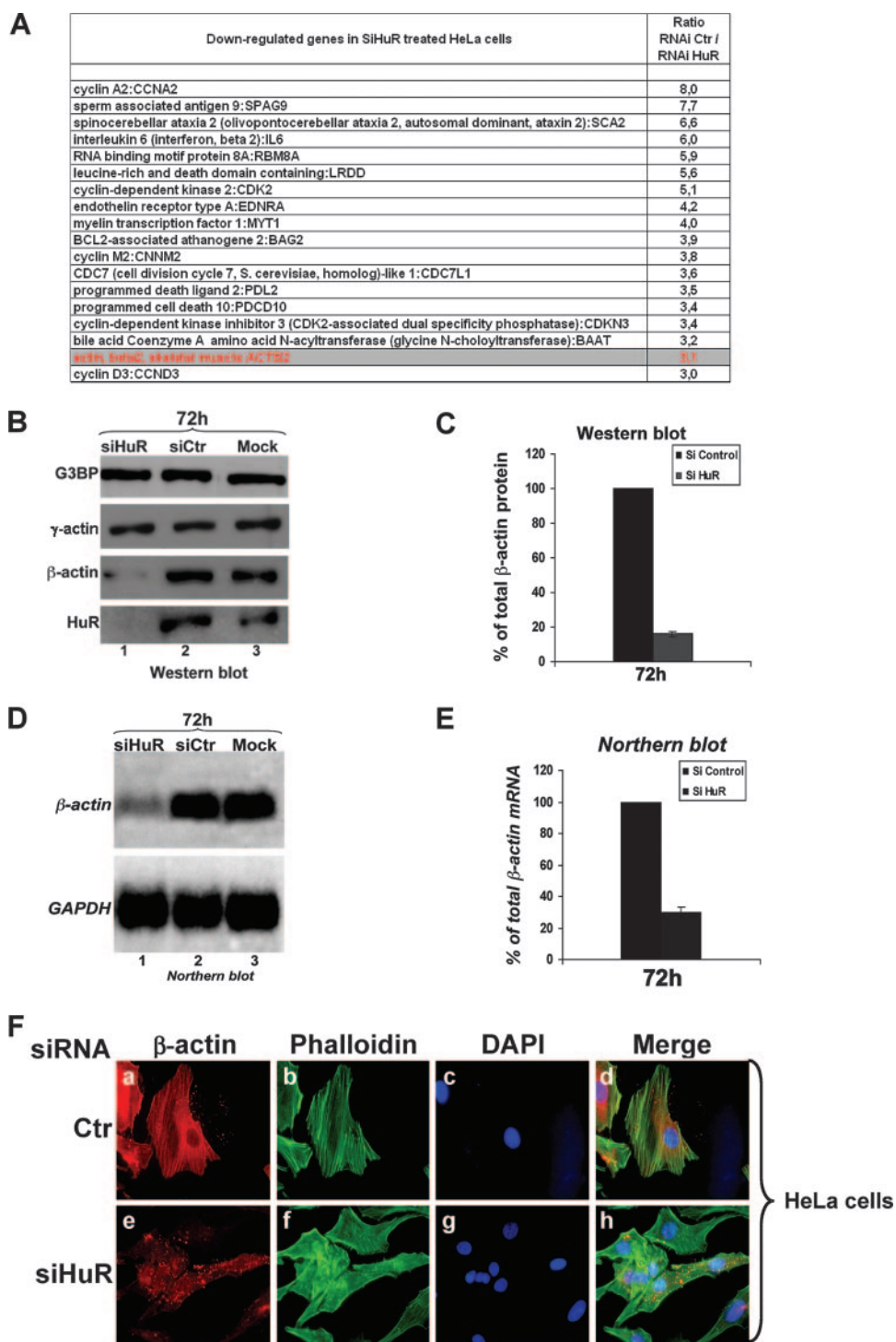| Down-regulated genes in SiHuR treated HeLa cells	Ratio RNAi Ctr / RNAi HuR
cyclin A2:CCNA2	8,0
sperm associated antigen 9:SPAG9	7,7
spinocerebellar ataxia 2 (olivopontocerebellar ataxia 2, autosomal dominant, ataxin 2):SCA2	6,6
interleukin 6 (interferon, beta 2):IL6	6,0
RNA binding motif protein 8A:RBM8A	5,9
leucine-rich and death domain containing:LRDD	5,6
cyclin-dependent kinase 2:CDK2	5,1
endothelin receptor type A:EDNRA	4,2
myelin transcription factor 1:MYT1	4,0
BCL2-associated athanogene 2:BAG2	3,9
cyclin M2:CNNM2	3,8
CDC7 (cell division cycle 7, S. cerevisiae, homolog)-like 1:CDC7L1	3,6
programmed death ligand 2:PDL2	3,5
programmed cell death 10:PDCD10	3,4
cyclin-dependent kinase inhibitor 3 (CDK2-associated dual specificity phosphatase):CDKN3	3,4
bile acid Coenzyme A amino acid N-acyltransferase (glycine N-choloyltransferase):BAAT	3,2
actin, beta2, skeletal muscle:ACTB2	3,1
cyclin D3:CCND3	3,0

FIG. 3. HuR knockdown leads to a decreased expression of beta-actin mRNA and protein. (A) cDNA microarray analysis of siRNA-treated HeLa cells. HeLa cells were grown at 37°C and treated with siHuR or siCtr. RNAs extracted from these cells were then processed using the standard protocol of the Health Network Microarray Center, Ontario Cancer Institute, hybridized to the 19,000 single-spotted human arrays. The CHIP files generated were then imported into GeneSpring v.6.5 (Silicon Genetics) to identify changes in gene expression. A default external background setting was used in conjunction with a gene-based background signal threshold to determine gene signal significance. The *n*-fold increase of a down regulated mRNA in siHuR-treated cells was calculated in comparison with the expression level of the same message in siCtr-treated cells. RNA for a gene was considered to be down regulated if the intensity of its signal was determined to be >3-fold less than that in the siCtr-treated cells. Overlay comparisons of cDNA array images were generated using an average of all of the gene signals on an array (siHuR or siCtr) to normalize the signal intensity to another array (global normalization). The mRNA values listed in this table represent the average for the affected messages in two independent experiments. (B) RNAi-mediated HuR knockdown in HeLa cells leads to decrease in β-actin protein level. Exponentially growing HeLa cells were treated with HuR RNAi duplexes siHuR, siCtr, or no RNAi (Mock). Seventy-two hours after transfection of RNAi duplexes, total cell extracts were prepared and β-actin protein was detected by Western blotting using an anti-β-actin

that is flexible enough to allow shape change without affecting its general structure (65). This feature is ensured by a solid network of cytoplasmic stress fibers that connect different points at the cellular edges, leading to the maintenance of cell-cell or cell-extracellular matrix contacts (9, 32). Using a siRNA experiment as described above, we investigated the effect of HuR on the distribution of these stress fibers. Seventy-two hours after the transfection of the siRNA duplexes, HeLa cells were fixed and processed for indirect immunofluorescence with an antibody against HuR (Fig. 2C, panels a and e) together with phalloidin to visualize stress fibers that are represented by polymerized F-actin proteins (Fig. 2C, panels b and f). Depleting the expression of HuR by using siHuR duplexes resulted in a significant reduction in stress fiber formation (Fig. 2C), however, the siCtr had no apparent effect. These results suggested that HuR is involved in the formation of a functional stress fiber network.

HuR knockdown leads to a decrease in expression of beta-actin protein and mRNA. The data described above reveal that the HuR protein is involved in cytoskeleton-based functions, such as cell adhesion, migration, and invasion. It is well established that HuR affects cell metabolism by regulating the stability and/or the movement of its mRNA targets (6, 17, 24). Therefore, it is possible that the role of HuR in cell behavior is mediated by its ability to regulate posttranscriptionally the expression of some mRNAs encoding key components of the cytoskeleton structures. To verify this possibility, we analyzed genome-wide expression profiles of wild-type and HuR knockdown HeLa cells. Cytoplasmic RNA was extracted from siHuR- or siCtr-treated cells and hybridized to human arrays, which contain 19,000 probe sets of characterized and unknown expressed sequence tags. Data from two independent experiments were averaged and filtered so that the n-fold change between wild-type and knockdown HuR cells was greater than or equal to 3. Comparison between siHuR- and siCtr-treated cells revealed a change in the expression of only a small fraction of total genes present on the arrays (<20) (Fig. 3A). Interestingly, we observed that the expression of the *beta-actin* (β-*actin*) mRNA, a major component of cytoskeleton-based functions (27–29), was down regulated by >3-fold in the absence of HuR. Thus, these data suggested that the β-*actin* mRNA could represent one of the main mRNA targets through which HuR affects cell behavior.

To validate the microarray data and to determine the exact level at which HuR affects the expression of the β-*actin* mRNA, we used RNA interference to specifically deplete the HuR protein. HeLa cells were transfected either with siCtr or siHuR, and then 72 h later they were collected and used for Western and Northern blot analyses. Unlike the case with γ-actin (34) or G3BP proteins (23), the level of β-actin protein

significantly decreased (by >70%) in siHuR-treated cells compared to that for the controls (Fig. 3B and C). Since the anti-β-actin antibodies used in these experiments were highly sensitive, the effect of HuR knockdown on the expression of β-actin protein was clearly visible only when we used 3 to 5 μg of total cell extract. These amounts are significantly smaller than the amounts used by other laboratories in experiments where they depleted the expression of HuR and used β-actin protein as a negative control (38, 44, 70, 74). This difference in the amount of total extracts employed explains why the effect of HuR on the expression of β-actin has never been reported before. Furthermore, our Northern blot analysis showed that depleting the expression of HuR in HeLa cells also significantly reduced the steady-state levels of β-*actin* mRNA (>65%) (Fig. 3D and E). The effect of HuR on β-actin expression was further confirmed by immunofluorescence experiments using the anti-β-actin antibody with HeLa cells treated with siHuR or siCtr (Fig. 3F). We observed a significant reduction in the levels of β-actin protein in HuR-knockdown HeLa cells compared to those for the control (Fig. 3F, panels a and e). Since similar results were obtained with WI-38 human fibroblasts (nontransformed cells) (see Fig. S1A, B, and C in the supplemental material) and IDH4 cells (transformed cells) (data not shown), we concluded that HuR affected cytoskeleton-based function by posttranscriptionally regulating the expression of the β-*actin* mRNA.

To assess whether depleting the expression of β-actin itself could show the same defects in cell behavior as those treated with siHuR duplexes, HeLa cells were transfected with siβ-actin or siCtr as described previously (31), and the effects of β-actin knockdown on stress fiber, cell migration, and cell adhesion were defined as described above. We observed that knocking down β-actin protein by >60% (Fig. 4A, compare lanes 1 and 2) resulted in a significant reduction in stress fiber formation (Fig. 4B) and a ~50% decrease in both cell migration (Fig. 4C and D) and cell adhesion (Fig. 4E and F). The effects of β-actin knockdown are consistent with previously published data (31, 46). These observations showed that depleting β-*actin* mRNA is sufficient to induce the same changes in cell behavior that were observed with HuR knockdown. Although these results further support the idea that HuR affects cell physiology by modulating the expression of β-*actin* mRNA, it is still possible that other yet-unknown HuR mRNA targets could be associated with these effects.

HuR associates with β-*actin* mRNA in a U-rich-dependent manner. It was previously shown, using a cDNA microarray analysis and immunoprecipitation approach, that β-*actin* mRNA associates with the HuR protein with high affinity (63). We confirmed this association by immunoprecipitating HuR from total HeLa cell extracts using the monoclonal anti-HuR

monoclonal antibody. The expression of HuR was also detected using an anti-HuR monoclonal antibody to control for proper RNAi knockdown and the expression of γ-actin using a specific antibody for this isoform. The expression of G3BP is shown as a loading control. (C) Quantification of the level of β-actin protein. Results represent the means ± standard deviations for three independent experiments. (D) HuR knockdown in HeLa cells leads to a decrease in β-actin mRNA level. RNAi experiment was performed as described in the legend to panel B, total RNA was prepared, and β-*actin* mRNA was detected by Northern blotting using a ^{32}P-labeled cDNA probe. The expression of *GAPDH* mRNA was also detected using a ^{32}P-labeled cDNA probe and is shown as a marker for loading. (E) Quantification of the β-*actin* mRNA level. Results represent the means ± standard deviations for four independent experiments. (F) HeLa cells were transfected with siHuR or siCtr and then stained with anti-β-actin antibody and FITC-phalloidin.
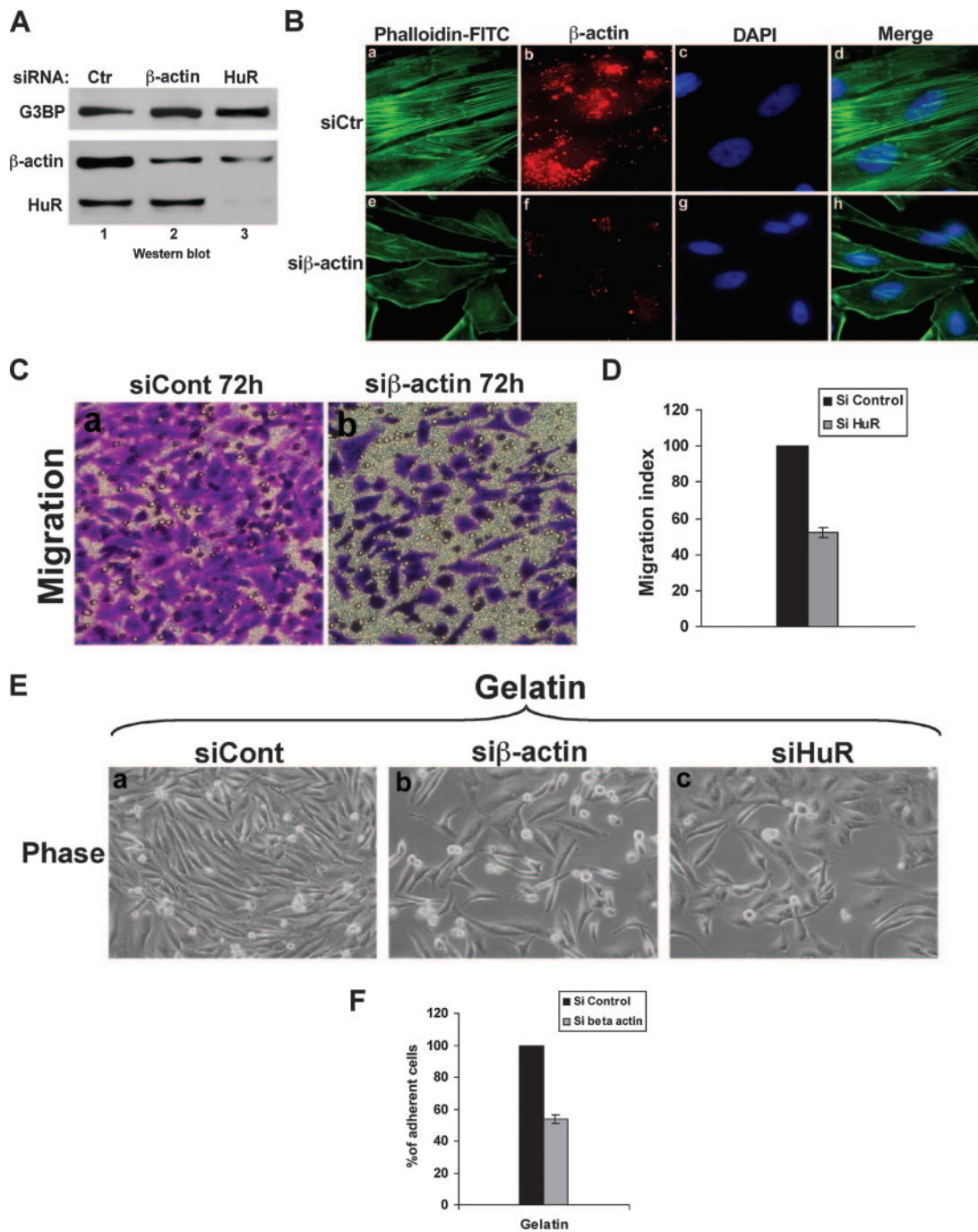
FIG. 4. Effects of β-actin knockdown on stress fiber formation, cell migration, and cell adhesion. (A) RNAi-mediated depletion of β-actin protein. Exponentially growing HeLa cells were treated with β-actin (siβ-actin), HuR (siHuR) RNAi duplexes, siCtr, or no RNAi (mock). Seventy-two hours after transfection of RNAi duplexes, total cell extracts were prepared and β-actin and HuR proteins were detected by Western blotting using anti-β-actin and -HuR monoclonal antibodies. The expression of the G3BP protein was also detected, using an anti-G3BP polyclonal antibody to control for proper RNAi knockdown. (B) Effect of β-actin knockdown on stress fiber formation. HeLa cells were transfected with siβ-actin or siCtr and then stained with the anti-β-actin antibody and FITC-phalloidin. (C and D) Effect of β-actin knockdown on cell migration. (C) Migration of HeLa cells treated with siβ-actin or siCtr was analyzed with an uncoated Boyden chamber. (D) Relative numbers of migrating cells are shown as means ± standard deviations for two experiments. For each experiment, pictures of 10 fields (equal sizes) were taken, and the cells have been counted. (E and F) Effect of β-actin knockdown on cell adhesion. (E) HeLa cells transfected with siCtr, siβ-actin, or siHuR were seeded on six-well plates with gelatin. Adherent cells were also stained with DAPI (data not shown). (F) Nuclei were counted by fluorescence microscopy. Relative numbers of cells are shown as means ± standard deviations for two experiments. For each experiment, pictures of 10 fields (equal sizes) were taken and the cells were counted.
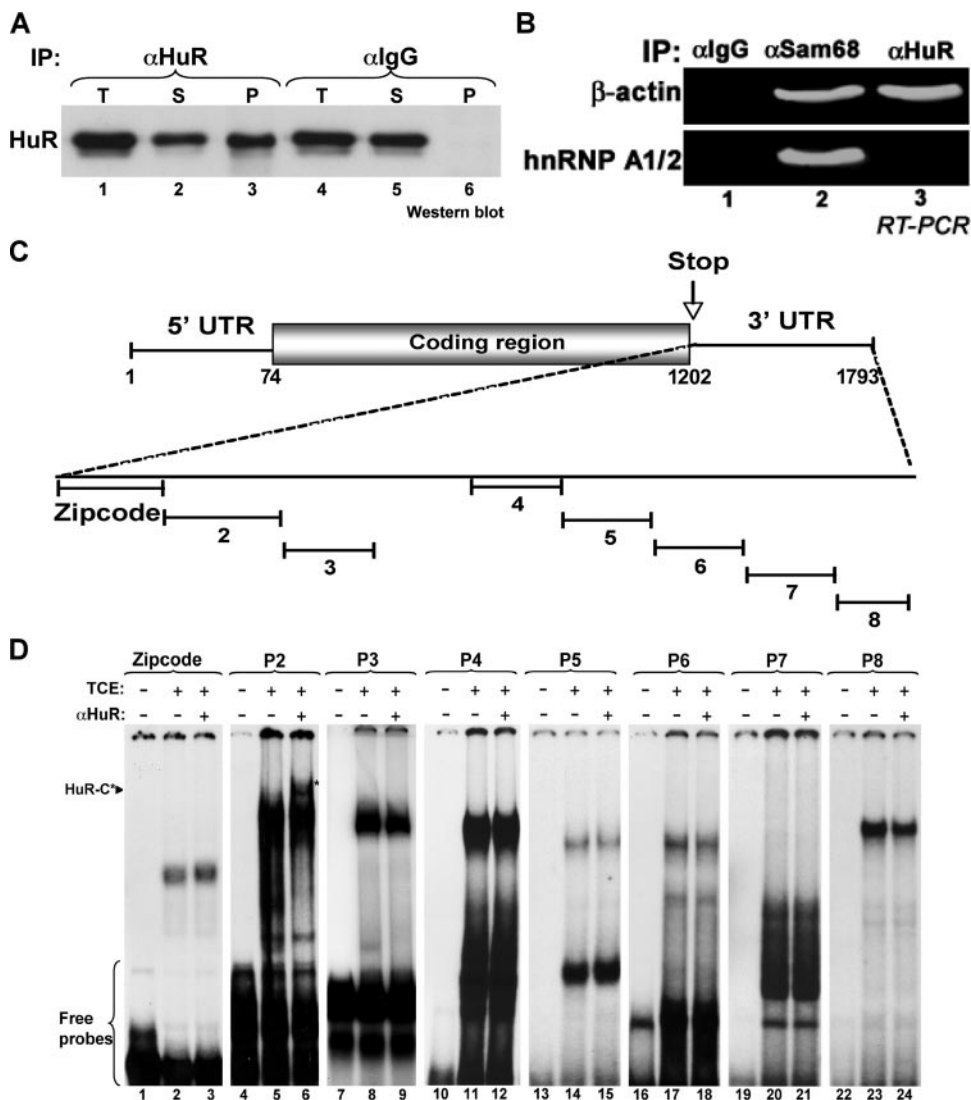
FIG. 5. HuR associates with β-*actin* mRNA through a U-rich element in the 3′UTR. (A) Immunoprecipitation (IP) of the HuR protein. HuR was immunoprecipitated from exponentially growing HeLa cells using an anti-HuR monoclonal antibody, and the presence of HuR in the immunoprecipitates (P) was assessed by immunoblotting using the same anti-HuR antibody. An anti-IgG monoclonal antibody was used as a negative control for the immunoprecipitation. The presence of HuR in total HeLa cell extracts (T), as well as in the flow-through (S) fraction, is shown. (B) β-*actin* mRNA associates with HuR protein. HuR was immunoprecipitated as described in panel A, and the presence of β-*actin* mRNA was assessed by RT-PCR. Anti-Sam68 and anti-IgG antibodies were used as positive and negative controls for the immunoprecipitation, respectively. (C) Schematic representation of the human β-*actin* cDNA and location of the eight regions within its 3′UTR that were used to generate radiolabeled RNA probes for RNA eletromobility shift assays. The accession number in the NCBI database of the β-*actin* mRNA sequence described in this figure is NM_001101. (D) HuR associates with β-*actin* mRNA through the p2 region. Gel shift binding assay performed by incubating TCE from HeLa cells with the radiolabeled β-*actin* mRNA probes listed in panel C. Supershift analysis was carried out where indicated (+ αHuR). HuR-C shows the supershifted complexes that contain the HuR protein.

antibody (22), and the presence of β-*actin* mRNA was assessed by reverse transcription (RT)-PCR. Western blot analysis showed that more than 50% of total cellular HuR was immunoprecipitated from HeLa cell extracts (Fig. 5A, lane 3, compared to lane 1). However, the immunoglobulin G (IgG) antibody was unable to cause HuR immunoprecipitation (lane 6, compared to lane 4). Furthermore, using RT-PCR analysis, we showed that β-*actin* mRNA was present only in HuR and Sam68 immunoprecipitates but not in the control (Fig. 5B, lanes 1 and 3, compared to lane 1). The *hnRNP A1* message, however, associated only with Sam68 (Fig. 5B, lane 2), which is

consistent with previously published data (36). Nucleotide sequence analysis of the β-*actin* mRNA revealed the presence of several U-rich elements in its 3′UTR. To delineate the exact HuR binding site (HuR-BS), we performed RNA electromobility shift assays using total extracts from HeLa cells and nine radiolabeled cRNA probes that covered the majority of the β-*actin* 3′UTR (Fig. 5C). When incubated with cell extracts, RNA-protein complexes were observed with all the cRNA probes tested (Fig. 5D). However, only the complex formed by probe 2 was supershifted to HuR complex (HuR-C) upon addition of the HuR antibody to the reaction mixture (Fig. 5D,
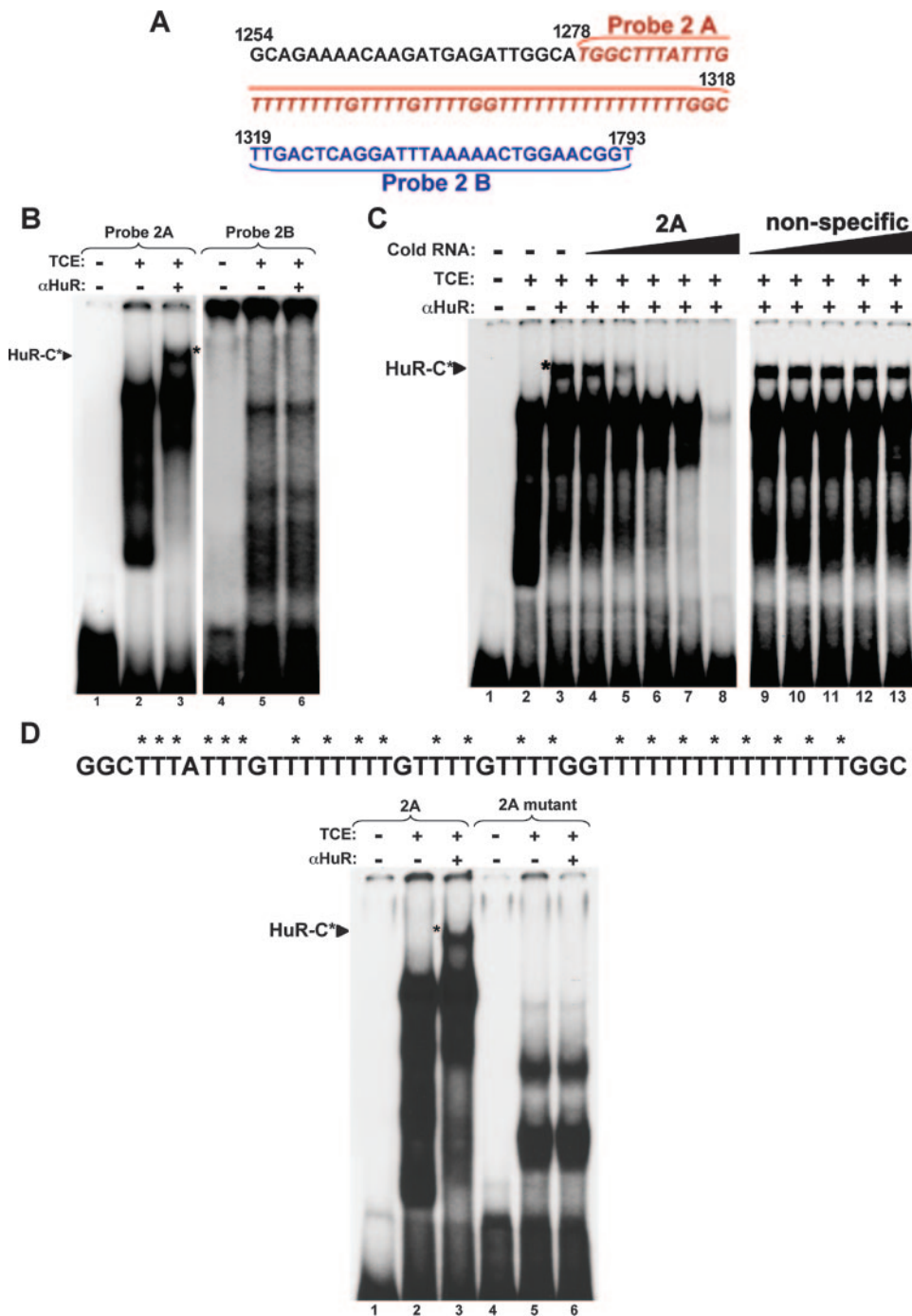
FIG. 6. Identification of HuR-binding site within the β-*actin* 3′UTR. (A) Nucleotide composition of the p2 element. Nucleotide sequence of the HuR-BS within the 3′UTR of β-*actin* (region 2) showing the two new probes (probes 2A and 2B) that were generated to identify the region of HuR binding. (B) HuR associates specifically with the 2A region. Gel shift binding assay performed by incubating TCE from HeLa cells with probe 2A (HuR-BS) and probe 2B. Supershift analysis was carried out where indicated (+ αHuR). The asterisk indicates the supershifted HuR-C complex. (C) Unlabeled 2A competes away the association of HuR with HuR-BS. Gel shift binding assay performed by incubating total cell extracts (TCE) from HeLa cells with radiolabeled probe 2A, as well as 1/10×, 1×, 10×, or 100× excess unlabeled probe 2A (specific) or probe 7 (nonspecific). Supershift analysis was carried out where indicated (+ αHuR). The asterisk shows supershifted complexes. (D) The 2A region but not the 2A mutant element associates with the HuR complex. Upper panel, nucleotide sequence of probe 2A showing the thymidine residues that were mutated to cytidine residues to generate mutant radiolabeled RNA probes for RNA eletromobility shift assays. The asterisk indicates the mutated residues. Lower panel, gel shift binding assay performed by incubating TCE from HeLa cells with radiolabeled probe 2A or mutant probe 2A. Supershift analysis was carried out where indicated (+ αHuR). The arrowhead shows supershifted complexes.

lane 6). Together these data indicated that the region covered by probe 2 contained the HuR-BS.

To define the exact nucleotide sequence of the HuR-BS within region 2, we generated two new radiolabeled cRNA probes, which we named 2A and 2B (Fig. 6A). Although both cRNA probes formed RNA-protein complexes when incubated with total cell extracts, only the complex formed by probe 2A was supershifted to form HuR-C upon addition of the HuR antibody to the reaction mixture (Fig. 6B, lane 3). To assess the binding specificity of HuR to probe 2A, competing unlabeled cRNA probes were used. Complex formation was inhibited when lysates were preincubated with 1-, 10-, or 100-fold excess of specific unlabeled probe 2A (Fig. 6C, lanes 6, 7, and 8). By contrast, similar *n*-fold excess of a nonspecific unlabeled cRNA probe (probe 6) failed to compete for binding (Fig. 6C, lanes 11, 12, and 13). Since region 2A is U rich, it was tempting to conclude that HuR associated specifically with the β-*actin* message in a U-rich-element-dependent manner. Therefore, to determine whether the U repeats in the 2A region were responsible for HuR binding, we generated a mutant probe where every other U in 2A was replaced by a cytidine residue (Fig. 6D, top panel). The use of this radiolabeled cRNA probe prevented the formation of the top RNA-protein complex, as well as the supershift observed upon addition of HuR antibodies to the reaction. (Fig. 6D, lanes 5 and 6). These data, combined with the fact that the recombinant GST-tagged HuR protein associated directly with the 2A cRNA probe in a gel shift assay (data not shown), suggested that HuR interacted directly with the 3′UTR of β-*actin* mRNA through a 50-nucleotide specific U-rich sequence.

To further delineate the HuR-BS within the 2A region, we performed the same electromobility shift assays as described above, this time using three overlapping radiolabeled cRNA probes, 2A left (2AL), 2A middle (2AM), and 2A right (2AR) (Fig. 7A), and the recombinant GST-tagged HuR protein (GST-HuR). When the three probes were incubated with GST-HuR, an RNA-binding complex was observed with the 2AR probe but not with the others (Fig. 7B, compares lanes 3 and 6 to lane 9). However, GST alone did not form a complex with any of these probes (Fig. 7B, lanes 2, 5, and 8). Of note, 2AM and 2AR have a common sequence, T_3GT_3GG, located, respectively, in their 3′ and 5′ ends (Fig. 7A). Since mutating the majority of the U located in 2AR at the same time (Fig. 6D) but not individually (data not shown) is required to prevent the association of 2AR with HuR, we concluded that the $T_{16}GGC$ sequence represented the minimum HuR-BS of the β-*actin* mRNA.

To determine whether 2AR mediates the interaction between HuR and the full-length (FL) β-*actin* mRNA, we used an unlabeled 2AR cRNA probe in a gel shift assay to compete away the association of HuR with an FL-radiolabeled β-actin 3′UTR. Complex formation between GST-HuR and the radiolabeled FL 3′UTR was significantly reduced, with a >10-fold excess of the specific unlabeled 2AR probe (Fig. 7C, lanes 13 and 14). By contrast, a similar *n*-fold excess of a nonspecific cRNA probe (probe 2AM) failed to compete for binding (Fig. 7C, lanes 7 and 8). These observations confirmed, in the context of the full-length 3′UTR, that the 2AR represented the functional HuR-BS in the β-*actin* mRNA.

The HuR protein mediates the stability but not the nuclear/cytoplasmic distribution of β-*actin* mRNA. The HuR protein is known as a stabilizer and an adaptor for export of its mRNA targets, and these effects are often mediated by its ability to interact with an AU-rich sequence located in the 3′UTR of these messages (6, 24). The observations described above suggested that HuR could affect the stability and/or the nuclear/cytoplasmic distribution of the β-*actin* mRNA through its interaction with the 2AR element. To distinguish between these two possibilities regarding the posttranscriptional effect of HuR on β-*actin* mRNA expression, we first tested the mRNA nuclear/cytoplasmic distribution. Total extracts from siHuR- and siCtr-treated cells were separated into cytoplasmic and nuclear fractions (see Fig. S2A and B in the supplemental material). The distribution of β-*actin* mRNA between these two fractions was then determined by Northern blot analysis using a radiolabeled probe (see Fig. S2C in the supplemental material). A greater than 70% knockdown in HuR expression was typically observed in these experiments, as shown by immunoblotting using the anti-HuR antibody (see Fig. S2A in the supplemental material). The quality of the cytoplasmic and nuclear fractions was also monitored by Western blotting using antitubulin (cytoplasmic marker) and anti-hnRNPA1 (nuclear marker) antibodies (15) (see Fig. S2B in the supplemental material). As expected, HuR knockdown resulted in a >65% decrease in the expression of β-*actin* mRNA (see Fig. S2C in the supplemental material). However, the slight accumulation of β-*actin* mRNA seen in the nucleus of siHuR-transfected cells was not statistically significant (see Fig. S2C and D in the supplemental material). Thus, it is unlikely that HuR is involved in the nuclear/cytoplasmic distribution of β-*actin* mRNA.

To test the effect of HuR on the stability of the β-*actin* mRNA, we performed ActD pulse-chase experiments on siHuR- and siCtr-treated HeLa cells (15). These cells were incubated in medium containing 5 μg/ml of the general transcriptional inhibitor ActD, and total RNA was collected at the indicated time points for analysis by Northern blotting using radiolabeled probes against β-*actin* and *GAPDH* messages. HuR knockdown resulted in a more than twofold decrease in the β-*actin* mRNA half-life compared to results with the control (Fig. 8A). The half-life of the β-*actin* message went from 8 h in control RNAi-treated cells to approximately 4 h in HuR RNAi-treated cells (Fig. 8B). These observations indicated that the well-known long half-life of β-*actin* mRNA depends on the expression of the HuR protein. Therefore, it is reasonable to assume that HuR could have a general effect on cell movement, adhesion, and growth by regulating actin-based cytoskeletal functions.

To confirm that the HuR-dependent stabilization of the β-*actin* mRNA is in fact mediated by the HuR-BS located in the 2A region, we used a reporter cDNA encoding the *Renilla* luciferase (pRL) that we conjugated to the β-*actin* 3′UTR (*pRL-βact-3′UTR*) or the 2A region (*pRL-2A*) or 2Amut region (*pRL-2Amut*). We transfected these plasmids into HeLa cells, and 24 h later we tested the half-life of the *pRL* message using 5 μg/ml of ActD as described in the legend to Fig. 8. Total RNA was collected at the indicated time points for analysis by Northern blotting using radiolabeled probes against the *pRL* message. We observed that while the *pRL-βact-3′UTR*

FIG. 7. Defining the exact nucleotide sequence of the HuR-BS within the region 2A. (A) Scheme of the nucleotide sequence of the 2A region within the 3′UTR of β-actin. The three new probes, 2AL, 2AM, and 2AR, that cover the 2A region are shown. (B) HuR associates with the 2AR region but not with the 2AL or the 2AM region. Gel shift binding assay performed by incubating 500 ng of purified GST or GST-HuR protein with radiolabeled 2AL, 2AM, and 2AR. The HuR-complex is indicated (HuR-C). (C) The unlabeled 2AR but not the 2AM element is able to compete away the association of HuR with the full-length β-actin 3′UTR. Gel shift binding assay performed by incubating purified protein GST or GST-HuR with radiolabeled full-length 3′UTR, as well as a 1/10×, 1×, 10×, or 100× excess of unlabeled 2AR (specific) or 2AM (nonspecific). The asterisk shows the HuR-RNA complex.

and *pRL-2A* messages (which form a complex with the HuR protein in a gel shift assay [Fig. 5 and 6]) remain stable (half-life of >6 h), the stability of the *pRL-2Amut* message (which does not bind complexes containing HuR [Fig. 6D]) decreased progressively (half-life of ~6 h) (Fig. 9). Additionally, upon 6 h

of ActD treatment, the levels of *pRL-βact-3′UTR* and *pRL-2A* decreased by only ~10%; however, the levels of *pRL-2Amut* mRNA decreased by ~50% (Fig. 9A). Since the decay profile of *pRL-2Amut* mRNA is almost the same as that of the *pRL* message alone (data not shown), our results argue that the
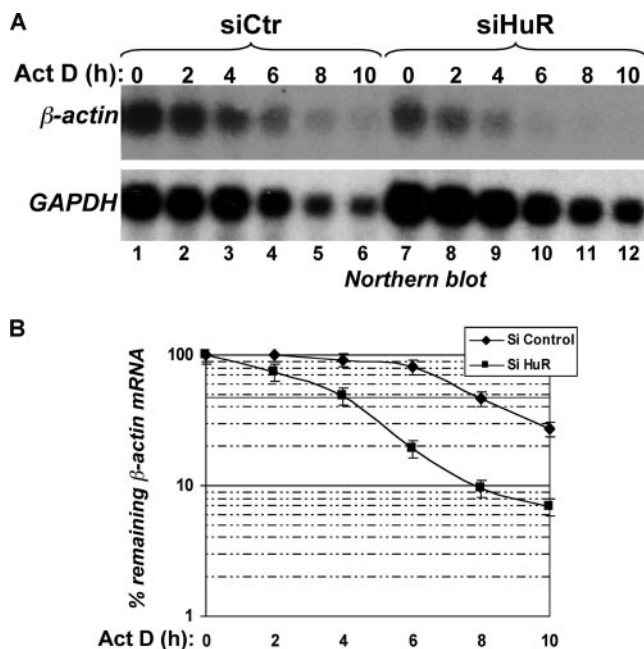
FIG. 8. RNAi-mediated HuR knockdown leads to a significant decrease in β-*actin* mRNA stability. (A) Role of HuR protein in β-*actin* mRNA stability. Exponentially growing HeLa cells were treated with siHuR or siCtr. Seventy-two hours after the RNAi transfection, 5 µg/ml of the transcriptional inhibitor ActD was added to the cell medium, and total RNA was prepared at the indicated times. The expression of β-*actin* mRNA (upper panel) or *GAPDH* message (lower panel) was detected using a ^{32}P-labeled cDNA probe. (B) Quantification of the half-life of β-*actin* mRNA in siHuR-treated cells compared to that in control RNAi-treated cells. Laser densitometric scanning of β-*actin* and *GAPDH* mRNAs was performed. β-*actin* mRNA levels were standardized against *GAPDH* levels and plotted as the percentage of remaining mRNA compared to message levels at time zero (where there is a 100% maximum mRNA level). Results represent the means ± standard deviations for three independent experiments.

HuR-BS located in the 2A region is likely to be responsible for the HuR-mediated long half-life of the β-*actin* message in vivo.

DISCUSSION

In the present study, we suggest that HuR affects cell behavior by regulating the stability of the β-*actin* mRNA. Although the direct link between the high expression levels of β-actin protein in all eukaryotic cells and the long half-life of its message is widely accepted (8, 50, 66), the regulatory mechanisms and the *cis*- and the *trans*-acting players involved in this effect have been elusive. Our data address this issue and demonstrate that HuR is responsible for the stabilization of the β-*actin* mRNA by associating with a *cis*-acting element, HuR-BS, which is a U-rich sequence located near the zip code (Fig. 5 to 8). Through this stabilization effect, HuR participates in key cellular actin-dependent physiological processes, such as the maintenance of an intact stress fiber network, as well as cell adhesion, cell migration, and cell invasion (Fig. 1 and 2). Together our results indicate that to maintain the high expression levels of β-actin protein that are needed for cytoskeleton-related cellular functions, the cell stabilizes β-*actin* mRNA through a specific association between HuR and a U-rich sequence within the β-*actin* 3′UTR (HuR-BS).

Previously it was shown that under conditions where actin assembly is blocked, the expression of β-*actin* mRNA decreases dramatically and this effect does not result from a reduction in the transcription rate of the *beta-actin* gene (4, 50, 51). These data, however, did not define the *cis*- and *trans*-

acting factors responsible for the well-known long half-life of this message. Since HuR has been known to stabilize mainly short-lived mRNAs that are required for cell cycle progression and cell differentiation (2, 19, 45, 67, 68, 69), it was unexpected to find that HuR is also responsible for the stabilization of the β-*actin* mRNA. HuR has been known to protect its mRNA targets from decay by associating with a destabilizing sequence, AU_3A (ARE), that localizes in the 3′UTR of these messages (6, 37, 61). ARE-containing messages are very unstable and can rapidly fluctuate in response to external stimuli (6, 37, 61). Since they encode key cell growth and differentiation factors, this rapid degradation process is crucial in maintaining a precise concentration of these proteins in order to protect the cell from uncontrolled growth. AREs have been classified into three categories based on their sequence (12). Class I AREs contain one to three copies of the sequence AUUUA, Class II AREs contain at least two overlapping copies of the sequence UUAUUUA(U/A)(U/A), and class III AREs contain U-rich sequences. HuR was thought to interact with and stabilize messages that contain mostly class I and II AREs (17, 53). Our results, showing that the nucleotide sequence of HuR-BS is U rich (Fig. 5 to 7), are consistent with those of a recent study, in which the binding sites of HuR in many of its mRNA targets have been identified as more U rich than AU rich (47). Thus, it is possible that the long stretch of 16 U's in the HuR-BS (Fig. 7) could explain in part why HuR maintains a tight association with the β-*actin* mRNA. However, we do not know whether this association is stable throughout the life span of a cell. Knocking down HuR in differentiated cells, such as skeletal
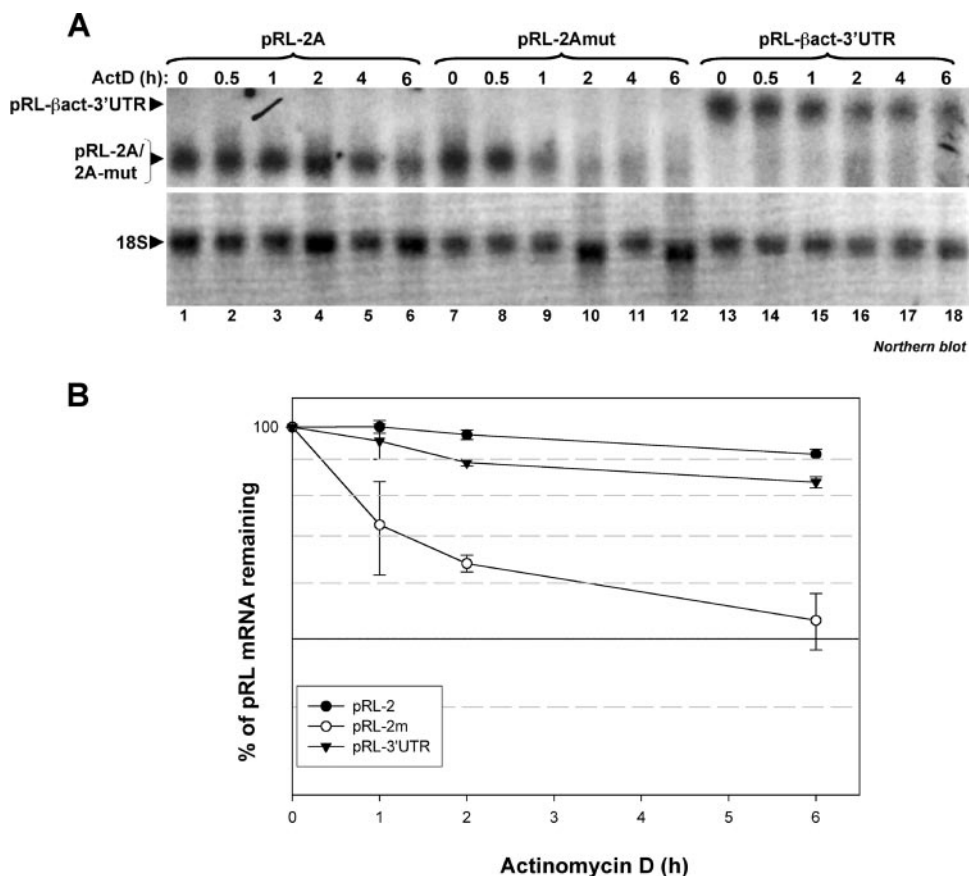
FIG. 9. The HuR-BS located in the 2A region, as well as the β-*actin*-3′UTR, increases the half-life of the *Renilla* luciferase (pRL) reporter message. (A) The 2AR mutant that does not bind to HuR in a gel shift assay is not able to stabilize the pRL mRNA. Exponentially growing HeLa cells were transfected with a cDNA encoding for *Renilla* luciferase (*pRL*) under the control of the simian virus 40 promoter, in which we cloned downstream of the stop codon the β-*actin* 3′UTR or the 2AR or 2AR-mut sequence. Twenty-four hours posttransfection, 5 μg/ml of the transcriptional inhibitor ActD was added to the cell medium and total RNA was prepared at the indicated times. The expression of *pRL* mRNA (upper panel) was detected using a ^{32}P-labeled cDNA probe. *18S* was used as a control for loading. (B) Quantification of the half-life of the *pRL* mRNA. Laser densitometric scanning of *pRL* mRNA was performed. *pRL* mRNA levels were standardized against those of *18S* and plotted as the percentage of remaining mRNA compared to message levels at time zero (where there are 100% maximum mRNA levels).

muscle fibers, could help in assessing the importance of a stable HuR-β-*actin* mRNA complex in maintaining tissue integrity in vivo.

An interesting attribute of β-*actin* mRNA is its targeted localization to the leading edge of polarized cells, such as chicken embryo fibroblasts, 3T3 fibroblasts, and endothelial cells (14). In chicken embryo fibroblasts, the cellular distribution of β-*actin* mRNA involves a 52-nucleotide sequence within its 3′UTR referred to as the zip code (39, 40). In addition, proteins such as ZBP1 (57) and ZBP2 (14) directly regulate the localization of β-*actin* mRNA by binding to the zip code. In the present study, we identify the HuR-BS within the β-*actin* mRNA as the region adjacent to the zip code (Fig. 5). The proximity of HuR-BS to the zip code raised the possibility that HuR could collaborate with ZBP proteins to regulate the nuclear/cytoplasmic distribution of β-*actin* mRNA. Indeed, the implication of HuR in mRNA export has been suggested by several studies (21, 24). Our data, however, indicate that the function of HuR is likely to be independent from the ZBPs. This conclusion is supported by our observations showing that HuR is not part of the zip code-binding proteins (Fig. 5D), and

its knockdown affects the half-life (Fig. 8) but not the nuclear/cytoplasmic distribution of the β-*actin* mRNA (see Fig. S2 in the supplemental material). These results are consistent with the fact that none of the ELAV-family proteins have been found in the ZBP complex (56). However, other studies have shown a direct link between depolymerization of the actin filaments and a 3′UTR-mediated rapid decay of β-*actin* mRNA (50). Thus, it is possible that under conditions where the actin filament network is disrupted, the association between HuR and the β-*actin* message is affected. Testing this possibility will help to better define how the cell integrates HuR-dependent posttranscriptional regulatory events and the actin-based cytoskeleton remodelling signals.

Because HuR levels increase significantly in many cancer cells (33) and its implication in regulating the expression of key cell cycle players has been suggested by several groups (2, 45, 68, 69), it was concluded that HuR plays a major role in cell transformation and malignancy. Since no direct experimental evidences were available linking HuR to these phenomena, it was important to test the effect of its depletion on β-*actin*-based cytoskeleton functions, such as cell migration, cell ad-

hesion, and cell invasion. Recent data have suggested a link between the strength of cell adhesion and the velocity by which the cell migrates inside an organ (28, 60). It is now well accepted that the two main features of cancer cells are uncontrolled proliferation and invasion (30). Malignant cells acquire the ability to spread throughout an organism, causing metastasis. This effect is linked to the reorganization of the actin cytoskeleton matrix, resulting in an increase in cell migration and invasion (73). Therefore, delineating the molecular mechanisms that regulate the expression of the β-actin protein is an important step that will help define how and why a cell acquires a transformation phenotype. Our data show that HuR deficiency causes impairments in cell adhesion, migration, and invasion and that these defects correlate with a loss of stress fibers (Fig. 1 and 2) (see Fig. S1 in the supplemental material). The stress fiber network is essential to synchronizing the tension distribution within a multicellular tissue through the forces they exercise on cell-cell and cell-ECM contacts (65). Therefore, our findings raise the possibility that the observed increase of the HuR expression level in several cancer cells (25, 33) enhances the expression of the β-actin protein, which in turn affects cytoskeleton organization. Hence, defining HuR as one of the key players that regulate actin-based cytoskeleton structures provides the possibility of controlling the migration and the invasion of cancer cells by modulating the expression of the HuR protein.

ACKNOWLEDGMENTS

REFERENCES

1. **Antic, D., and J. D. Keene.** 1997. Embryonic lethal abnormal visual RNA-binding proteins involved in growth, differentiation, and posttranscriptional gene expression. Am. J. Hum. Genet. **61:**273–278.
2. **Atasoy, U., J. Watson, D. Patel, and J. D. Keene.** 1998. ELAV protein HuA (HuR) can redistribute between nucleus and cytoplasm and is upregulated during serum stimulation and T cell activation. J. Cell Sci. **111:**3145–3156.
3. **Bassell, G., and R. H. Singer.** 1997. mRNA and cytoskeletal filaments. Curr. Opin. Cell Biol. **9:**109–115.
4. **Bershadsky, A. D., U. Gluck, O. N. Denisenko, T. V. Sklyarova, I. Spector, and A. Ben-Ze'ev.** 1995. The state of actin assembly regulates actin and vinculin expression by a feedback loop. J. Cell Sci. **108:**1183–1193.
5. **Brennan, C. M., I. E. Gallouzi, and J. A. Steitz.** 2000. Protein ligands to HuR modulate its interaction with target mRNAs in vivo. J. Cell Biol. **151:**1–14.
6. **Brennan, C. M., and J. A. Steitz.** 2001. HuR and mRNA stability. Cell. Mol. Life Sci. **58:**266–277.
7. **Buhrer, C., J. Atzpodien, S. Oz, and G. Henze.** 1991. Fosfomycin does not reduce cytostatic activity of cis-platinum against human osteosarcoma cell lines in vitro. Pediatr. Hematol. Oncol. **8:**243–249.
8. **Bulinski, J. C.** 2006. Cell biology. Actin discrimination. Science **313:**180–181.
9. **Burridge, K., and K. Wennerberg.** 2004. Rho and Rac take center stage. Cell **116:**167–179.
10. **Carlsson, F., and E. J. Brown.** 2006. Actin-based motility of intracellular bacteria, and polarized surface distribution of the bacterial effector molecules. J. Cell Physiol. **209:**288–296.
11. **Chartrand, P., R. H. Singer, and R. M. Long.** 2001. RNP localization and transport in yeast. Annu. Rev. Cell Dev. Biol. **17:**297–310.
12. **Chen, C. Y., and A. B. Shyu.** 1995. AU-rich elements: characterization and importance in mRNA degradation. Trends Biochem. Sci. **20:**465–470.
13. **Chen, H., B. W. Bernstein, and J. R. Bamburg.** 2000. Regulating actin-filament dynamics in vivo. Trends Biochem. Sci. **25:**19–23.
14. **Condeelis, J., and R. H. Singer.** 2005. How and why does beta-actin mRNA target? Biol. Cell **97:**97–110.
15. **Di Marco, S., R. Mazroui, P. Dallaire, S. Chittur, S. A. Tenenbaum, D. Radzioch, A. Marette, and I. E. Gallouzi.** 2005. NF-κB-mediated MyoD decay during muscle wasting requires nitric oxide synthase mRNA stabilization, HuR protein, and nitric oxide release. Mol. Cell. Biol. **25:**6533–6545.
16. **Fan, X. C., and J. A. Steitz.** 1998. HNS, a nuclear-cytoplasmic shuttling sequence in HuR. Proc. Natl. Acad. Sci. USA **95:**15293–15298.
17. **Fan, X. C., and J. A. Steitz.** 1998. Overexpression of HuR, a nuclear-cytoplasmic shuttling protein, increases the in vivo stability of ARE-containing mRNAs. EMBO J. **17:**3448–3460.
18. **Farina, K. L., S. Huttelmaier, K. Musunuru, R. Darnell, and R. H. Singer.** 2003. Two ZBP1 KH domains facilitate beta-actin mRNA localization, granule formation, and cytoskeletal attachment. J. Cell Biol. **160:**77–87.
19. **Figueroa, A., A. Cuadrado, J. Fan, U. Atasoy, G. E. Muscat, P. Munoz-Canoves, M. Gorospe, and A. Munoz.** 2003. Role of HuR in skeletal myogenesis through coordinate regulation of muscle differentiation genes. Mol. Cell. Biol. **23:**4991–5004.
20. **Gallin, J. I., J. A. Klimerman, G. A. Padgett, and S. M. Wolff.** 1975. Defective mononuclear leukocyte chemotaxis in the Chediak-Higashi syndrome of humans, mink, and cattle. Blood **45:**863–870.
21. **Gallouzi, I. E., and C. M. Brennan, and J. A. Steitz.** 2001. Protein ligands mediate the CRM1-dependent export of HuR in response to heat shock. RNA **7:**1348–1361.
22. **Gallouzi, I. E., C. M. Brennan, M. G. Stenberg, M. S. Swanson, A. Eversole, N. Maizels, and J. A. Steitz.** 2000. HuR binding to cytoplasmic mRNA is perturbed by heat shock. Proc. Natl. Acad. Sci. USA **97:**3073–3078.
23. **Gallouzi, I. E., F. Parker, K. Chebli, F. Maurier, E. Labourier, I. Barlat, J. P. Capony, B. Tocque, and J. Tazi.** 1998. A novel phosphorylation-dependent RNase activity of GAP-SH3 binding protein: a potential link between signal transduction and RNA stability. Mol. Cell. Biol. **18:**3956–3965.
24. **Gallouzi, I. E., and J. A. Steitz.** 2001. Delineation of mRNA export pathways by the use of cell-permeable peptides. Science **294:**1895–1901.
25. **Gorospe, M.** 2003. HuR in the mammalian genotoxic response: post-transcriptional multitasking. Cell Cycle **2:**412–414.
26. **Gumbiner, B. M.** 1996. Cell adhesion: the molecular basis of tissue architecture and morphogenesis. Cell **84:**345–357.
27. **Gupton, S. L., K. L. Anderson, T. P. Kole, R. S. Fischer, A. Ponti, S. E. Hitchcock-DeGregori, G. Danuser, V. M. Fowler, D. Wirtz, D. Hanein, and C. M. Waterman-Storer.** 2005. Cell migration without a lamellipodium: translation of actin dynamics into cell movement mediated by tropomyosin. J. Cell Biol. **168:**619–631.
28. **Gupton, S. L., and C. M. Waterman-Storer.** 2006. Spatiotemporal feedback between actomyosin and focal-adhesion systems optimizes rapid cell migration. Cell **125:**1361–1374.
29. **Hall, A.** 2005. Rho GTPases and the control of cell behaviour. Biochem. Soc. Trans. **33:**891–895.
30. **Hanahan, D., and R. A. Weinberg.** 2000. The hallmarks of cancer. Cell **100:**57–70.
31. **Harborth, J., S. M. Elbashir, K. Bechert, T. Tuschl, and K. Weber.** 2001. Identification of essential genes in cultured mammalian cells using small interfering RNAs. J. Cell Sci. **114:**4557–4565.
32. **Harris, A. K., D. Stopak, and P. Wild.** 1981. Fibroblast traction as a mechanism for collagen morphogenesis. Nature **290:**249–251.
33. **Heinonen, M., P. Bono, K. Narko, S. H. Chang, J. Lundin, H. Joensuu, H. Furneaux, T. Hla, C. Haglund, and A. Ristimaki.** 2005. Cytoplasmic HuR expression is a prognostic factor in invasive ductal breast carcinoma. Cancer Res. **65:**2157–2161.
34. **Herman, I. M.** 1993. Actin isoforms. Curr. Opin. Cell Biol. **5:**48–55.
35. **Hoock, T. C., P. M. Newcomb, and I. M. Herman.** 1991. Beta actin and its mRNA are localized at the plasma membrane and the regions of moving cytoplasm during the cellular response to injury. J. Cell Biol. **112:**653–664.
36. **Itoh, M., I. Haga, Q. H. Li, and J. Fujisawa.** 2002. Identification of cellular mRNA targets for RNA-binding protein Sam68. Nucleic Acids Res. **30:**5452–5464.
37. **Jacobson, A., and S. W. Peltz.** 1996. Interrelationships of the pathways of mRNA decay and translation in eukaryotic cells. Annu. Rev. Biochem. **65:**693–739.
38. **Kawai, T., A. Lal, X. Yang, S. Galban, K. Mazan-Mamczarz, and M. Gorospe.** 2006. Translational control of cytochrome *c* by RNA-binding proteins TIA-1 and HuR. Mol. Cell. Biol. **26:**3295–3307.
39. **Kislauskis, E. H., Z. Li, R. H. Singer, and K. L. Taneja.** 1993. Isoform-specific 3′-untranslated sequences sort alpha-cardiac and beta-cytoplasmic actin messenger RNAs to different cytoplasmic compartments. J. Cell Biol. **123:**165–172.
40. **Kislauskis, E. H., X. Zhu, and R. H. Singer.** 1994. Sequences responsible for intracellular localization of beta-actin messenger RNA also affect cell phenotype. J. Cell Biol. **127:**441–451.
41. **Klemke, R. L., J. Leng, R. Molander, P. C. Brooks, K. Vuori, and D. A. Cheresh.** 1998. CAS/Crk coupling serves as a "molecular switch" for induction of cell migration. J. Cell Biol. **140:**961–972.
42. **Kullmann, M., U. Gopfert, B. Siewe, and L. Hengst.** 2002. ELAV/Hu proteins inhibit p27 translation via an IRES element in the p27 5′UTR. Genes Dev. **16:**3087–3099.
43. **Kurban, G., V. Hudon, E. Duplan, M. Ohh, and A. Pause.** 2006. Characterization of a von Hippel Lindau pathway involved in extracellular matrix remodeling, cell invasion, and angiogenesis. Cancer Res. **66:**1313–1319.
44. **Lal, A., T. Kawai, X. Yang, K. Mazan-Mamczarz, and M. Gorospe.** 2005.

Antiapoptotic function of RNA-binding protein HuR effected through pro-thymosin alpha. EMBO J. **24:**1852–1862.

45. **Lin, S., W. Wang, G. M. Wilson, X. Yang, G. Brewer, N. J. Holbrook, and M. Gorospe.** 2000. Down-regulation of cyclin D1 expression by prostaglandin A(2) is mediated by enhanced cyclin D1 mRNA turnover. Mol. Cell. Biol. **20:**7903–7913.

46. **Liu, N., K. Academia, T. Rubio, T. Wehr, T. Yeck, L. Jordan, K. Hamby, and A. Paulus.** 2007. Actin deficiency induces cofilin phosphorylation: proteome analysis of HeLa cells after beta-actin gene silencing. Cell Motil. Cytoskelet. **64:**110–120.

47. **Lopez de Silanes, I., J. Fan, C. J. Galban, R. G. Spencer, K. G. Becker, and M. Gorospe.** 2004. Global analysis of HuR-regulated gene expression in colon cancer systems of reducing complexity. Gene Expr. **12:**49–59.

48. **Lu, M. L., D. A. Beacham, and B. S. Jacobson.** 1989. The identification and characterization of collagen receptors involved in HeLa cell-substratum adhesion. J. Biol. Chem. **264:**13546–13558.

49. **Lu, M. L., R. J. McCarron, and B. S. Jacobson.** 1992. Initiation of HeLa cell adhesion to collagen is dependent upon collagen receptor upregulation, segregation to the basal plasma membrane, clustering and binding to the cytoskeleton. J. Cell Sci. **101:**873–883.

50. **Lyubimova, A., A. D. Bershadsky, and A. Ben-Ze'ev.** 1999. Autoregulation of actin synthesis requires the 3′-UTR of actin mRNA and protects cells from actin overproduction. J. Cell Biochem. **76:**1–12.

51. **Lyubimova, A., A. D. Bershadsky, and A. Ben-Ze'ev.** 1997. Autoregulation of actin synthesis responds to monomeric actin levels. J. Cell Biochem. **65:**469–478.

52. **Olave, I. A., S. L. Reck-Peterson, and G. R. Crabtree.** 2002. Nuclear actin and actin-related proteins in chromatin remodeling. Annu. Rev. Biochem. **71:**755–781.

53. **Peng, S. S., C. Y. Chen, N. Xu, and A. B. Shyu.** 1998. RNA stabilization by the AU-rich element binding protein, HuR, an ELAV protein. EMBO J. **17:**3461–3470.

54. **Percipalle, P., A. Jonsson, D. Nashchekin, C. Karlsson, T. Bergman, A. Guialis, and B. Daneholt.** 2002. Nuclear actin is associated with a specific subset of hnRNP A/B-type proteins. Nucleic Acids Res. **30:**1725–1734.

55. **Pollard, T. D., and J. A. Cooper.** 1986. Actin and actin-binding proteins. A critical evaluation of mechanisms and functions. Annu. Rev. Biochem. **55:**987–1035.

56. **Ross, A. F., Y. Oleynikov, E. H. Kislauskis, K. L. Taneja, and R. H. Singer.** 1997. Characterization of a beta-actin mRNA zipcode-binding protein. Mol. Cell. Biol. **17:**2158–2165.

57. **Ross, R. A., D. L. Lazarova, G. T. Manley, P. S. Smitt, B. A. Spengler, J. B. Posner, and J. L. Biedler.** 1997. HuD, a neuronal-specific RNA-binding protein, is a potential regulator of MYCN expression in human neuroblastoma cells. Eur. J. Cancer **33:**2071–2074.

58. **Sakai, T., S. Li, D. Docheva, C. Grashoff, K. Sakai, G. Kostka, A. Braun, A. Pfeifer, P. D. Yurchenco, and R. Fassler.** 2003. Integrin-linked kinase (ILK) is required for polarizing the epiblast, cell adhesion, and controlling actin accumulation. Genes Dev. **17:**926–940.

59. **Scheer, U., H. Hinssen, W. W. Franke, and B. M. Jockusch.** 1984. Microinjection of actin-binding proteins and actin antibodies demonstrates involvement of nuclear actin in transcription of lampbrush chromosomes. Cell **39:**111–122.

60. **Schwartz, M. A., and A. R. Horwitz.** 2006. Integrating adhesion, protrusion, and contraction during cell migration. Cell **125:**1223–1225.

61. **Shaw, G., and R. Kamen.** 1986. A conserved AU sequence from the 3′ untranslated region of GM-CSF mRNA mediates selective mRNA degradation. Cell **46:**659–667.

62. **Snee, M., G. J. Kidd, T. P. Munro, and R. Smith.** 2002. RNA trafficking and stabilization elements associate with multiple brain proteins. J. Cell Sci. **115:**4661–4669.

63. **Tenenbaum, S. A., C. C. Carson, P. J. Lager, and J. D. Keene.** 2000. Identifying mRNA subsets in messenger ribonucleoprotein complexes by using cDNA arrays. Proc. Natl. Acad. Sci. USA **97:**14085–14090.

64. **Tenenbaum, S. A., P. J. Lager, C. C. Carson, and J. D. Keene.** 2002. Ribonomics: identifying mRNA subsets in mRNP complexes using antibodies to RNA-binding proteins and genomic arrays. Methods **26:**191–198.

65. **Thery, M., A. Pepin, E. Dressaire, Y. Chen, and M. Bornens.** 2006. Cell distribution of stress fibres in response to the geometry of the adhesive environment. Cell Motil. Cytoskel. **63:**341–355.

66. **Vandekerckhove, J., and K. Weber.** 1978. At least six different actins are expressed in a higher mammal: an analysis based on the amino acid sequence of the amino-terminal tryptic peptide. J. Mol. Biol. **126:**783–802.

67. **van der Giessen, K., S. Di-Marco, E. Clair, and I. E. Gallouzi.** 2003. RNAi-mediated HuR depletion leads to the inhibition of muscle cell differentiation. J. Biol. Chem. **278:**47119–47128.

68. **Wang, W., M. C. Caldwell, S. Lin, H. Furneaux, and M. Gorospe.** 2000. HuR regulates cyclin A and cyclin B1 mRNA stability during cell proliferation. EMBO J. **19:**2340–2350.

69. **Wang, W., H. Furneaux, H. Cheng, M. C. Caldwell, D. Hutter, Y. Liu, N. Holbrook, and M. Gorospe.** 2000. HuR regulates p21 mRNA stabilization by UV light. Mol. Cell. Biol. **20:**760–769.

70. **Wang, W., X. Yang, I. Lopez de Silanes, D. Carling, and M. Gorospe.** 2003. Increased AMP:ATP ratio and AMP-activated protein kinase activity during cellular senescence linked to reduced HuR function. J. Biol. Chem. **278:**27016–27023.

71. **Welch, M. D.** 1999. The world according to Arp: regulation of actin nucleation by the Arp2/3 complex. Trends Cell. Biol. **9:**423–427.

72. **Welch, M. D., and R. D. Mullins.** 2002. Cellular control of actin nucleation. Annu. Rev. Cell Dev. Biol. **18:**247–288.

73. **Yamazaki, D., S. Kurisu, and T. Takenawa.** 2005. Regulation of cancer cell motility through actin reorganization. Cancer Sci. **96:**379–386.

74. **Zou, T., K. Mazan-Mamczarz, J. N. Rao, L. Liu, B. S. Marasa, A. H. Zhang, L. Xiao, R. Pullmann, M. Gorospe, and J. Y. Wang.** 2006. Polyamine depletion increases cytoplasmic levels of RNA-binding protein HuR leading to stabilization of nucleophosmin and p53 mRNAs. J. Biol. Chem. **281:**19387–19394.